ChemComm

Accepted Manuscript

This article can be cited before page numbers have been issued, to do this please use: H. Yang, Y. Li, D. Wang, Y. Liu, W. Wei, Y. Zhang, S. Liu and P. Li, *Chem. Commun.*, 2019, DOI: 10.1039/C9CC02610J.

ROYAL SOCIETY OF CHEMISTRY

rsc.li/chemcomm

ChemComm

View Article Online
DOI: 10.1039/C9CC02610J

COMMUNICATION

Quartz crystal microbalance for telomerase sensing based on gold nanoparticles induced signal amplification

Received 00th January 20xx,
Accepted 00th January 20xx

DOI: 10.1039/x0xx00000x

Haitang Yang[a], Ying Li[a], Dingzhong Wang[b], Yong Liu[c], Wei Wei[a,*], Yuanjian Zhang[a], Songqin Liu[a], and Peng Li[b,*].

A novel circulating-flow quartz crystal microbalance (QCM) biosensing method has been established to detect telomerase. Oligonucleotide-functionalized gold nanoparticles (GNPs-cDNA) have been used to amplify the frequency change, which make this QCM to be a sensitive biosensor for telomerase activity detection, The detection limit was as low as 37 cells/mL. The assay platform exhibited excellent selectivity.

Telomere maintenance has been shown to be essential for unlimited growth potential of human cells and is regarded as one hallmark of cancer. Telomerase contains an RNA component that has a template region complementary to $(TTAGGG)_n$ repeats that permits the synthesis of TTAGGG telomeric DNA onto chromosomal ends.[1] In normal eukaryotic cells, the catalytic component of telomerase is inhibited and telomere is shortened during cell division. When the telomere length reaches a critical point, the cells stop dividing and apoptotic. In 80-90% cancer cells, telomerase is detectable and the telomere length maintains stable, which leads to the stabilization of telomeres and confers immortality or unlimited growth potential.[2] Accurate and efficient determination of telomerase activity is significant. Conventionally, the polymerase chain reaction (PCR)-based telomerase assay called the TRAP (telomeric repeat amplification protocol) assay was used but relatively complicated.[3] To break the limitation, manifold alternative approaches for telomerase activity detection based on various unique probes have been developed.[4] Such as UV-Vis,[5-7] fluorescence,[8-13] electrochemistry,[14-18] surface-enhanced raman scattering (SERS),[19] circular dichroism (CD)[20] and so on.

These methods were primarily based on the following properties of the extended telomerase substrate (TS) primer (5'-AAT CCG TCG AGC AGA GTT $(TTAGGG)_n$-3'). Firstly, compared with TS primer, the extended TS primer has more negative charges which would change the interactions with signal probes. For example, AIEgens-based bioprobe for telomerase detection was a typical method.[12] Second, G-rich DNA sequences are known to form the catalytic hemin-G-quadruplex nanostructures in the presence of hemin. Freeman et al. reported the optical analysis of telomerase based on the G-quadruplex/hemin DNAzyme which catalyzed the H_2O_2-mediated oxidation of TMB.[21] Third, telomerase extension products can be used for DNA hybridization or strand displacement reaction, which are beneficial to construct biosensors. Ling et al. constructed an electrochemical sensor for telomerase detection based on the electrocatalysis of platinum nanoparticle (Pt NP) encapsulated metal-organic frameworks (MOFs).[22] After the TS primer was extended, the Pt@UiO-66-NH_2-cDNA probe could form a hybrid with the extended part on the sensor surface, resulting in the increasing electrocatalytic current towards $NaBH_4$ oxidation.

The quartz crystal microbalances (QCM) biosensor has been widely used in biochemical analysis as a real-time, label-free and mass-sensitive sensing platform.[23] The resonant frequency shifts (ΔF) of a piezoelectric crystal are directly proportional to the adsorbed mass according to the Sauerbrey equation.[24] Since the sensitivity is dissatisfactory especially for low mass biological molecules without further signal amplification. Gold nanoparticles (GNPs) were integrated into QCM as effective amplifiers in the DNA detection, as GNPs have relatively large mass and also are easy to functionalize.[25-28] For example, Chen et al. developed a highly sensitive QCM biosensor for protein using aptamer-functionalized GNPs for amplification.[28] Hao et al. constructed a DNA probe functionalized QCM biosensor which could specifically recognize the target DNA fragment of *B. anthracis*. GNPs

[a] *Jiangsu Engineering Laboratory of Smart Carbon-Rich Materials and Device, Jiangsu Province Hi-Tech Key Laboratory for Bio-medical Research, School of Chemistry and Chemical Engineering, Southeast University, Nanjing, 211189, China.*
[b] *Zhengzhou Tobacco Research Institute of CNTC, Zhengzhou 450001, China.*
[c] *College of Chemistry and Chemical Engineering, Henan University, Kaifeng, 475004, PR China.*
E-mail address: weiw@seu.edu.cn (W. Wei); Tel.: 86-25-52090613; Fax: 86-25-52090618.
†Electronic Supplementary Information (ESI) available: See DOI: 10.1039/x0xx00000x

functionalized DNA probe, complementary to the target DNA, was used to amplify the detection signal.[29]

In this work, we developed a highly sensitive QCM biosensor for telomerase detection. Gold nanoparticle functionalized DNA probe (GNPs-cDNA), complementary to the telomerase extension product, was used to amplify the detection signal. As shown in Scheme 1, TS primer was firstly immobilized on the chip surface by the Au-S affinity binding. Then, telomerase extract from A549 cells was added to telomerase extension reaction buffer containing dNTPs, it extended $(TTAGGG)_n$ on the 3' end of TS primer using deoxyribonucleoside triphosphates (dNTPs) as raw material. Finally, the GNPs-cDNA was added to hybridize with the extended sequences and resulted in the obvious Δ*F* for signal amplification. Using this strategy, the proposed method has the linear range from 100 cells/mL to 7800 cells/mL, with a detection limit of 37 cells/mL. High accuracy and reproducibility were obtained when it was used to detect telomerase in urine samples.

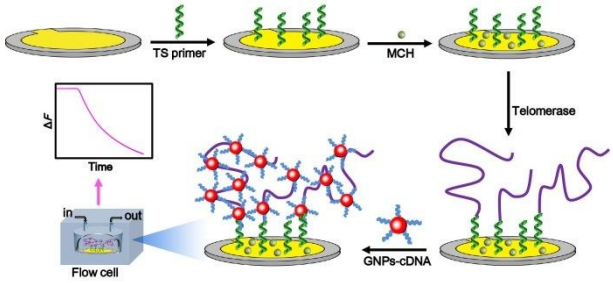

Scheme 1 Schematic representation of the sensing processes of QCM biosensor based on GNPs-cDNA induced signal amplification

The whole detection process and signal response were presented in Fig. 1. The real-time responses of this QCM biosensor to the TS modification, telomerization reaction and the amplifying signal by GNPs-cDNA were observed in detail. Buffer induced slightly change of frequency baseline. After addition of TS, the frequency decreased by 6.5 Hz. Then, MCH was used to block the remaining active sites. After flushing QCM surface with Tris-NaCl, telomerase extension reaction buffer was injected and the frequency increased slightly. Slight decrement of frequency occurred when dNTPs was injected. When telomerase solution consisting of dNTPs and telomerase originating from the specified number of cancer cells was introduced into the detection chamber, the repeats (TTAGGG)n were extended on the 3' end of TS primer using dNTPs as raw material. The formation of extended TS primer produced 12.06 Hz decrement for 3000 A549 cells/mL, which is not sensitive enough to be detected. After rinsing with Tris-NaCl buffer, the signal amplification was obtained by injecting the GNPs-cDNA into the chamber. The total frequency shift of GNPs-cDNA reached 100.9 Hz in 30 min, which account for the hybridization of GNPs-cDNA with extended TS primer. This signal amplification made this QCM biosensor sensitive enough for telomerase activity detection.

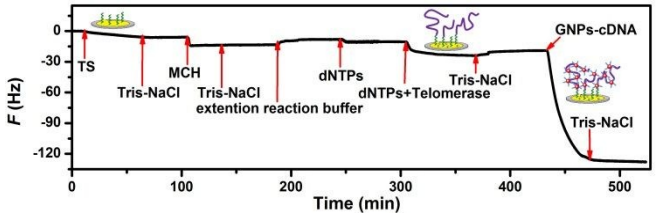

Fig. 1 Real-time response of the TS functionalized QCM biosensor to telomerization reaction and subsequent signal amplification by GNPs-cDNA.

The transmission electron microscopic (TEM) was used to characterize GNPs that was prepared according to the literature (Fig. 2A).[30] TEM image showed that GNPs were uniformly dispersed in solution. The distributions of particle size and their mean values (~13 nm) analyzed from the corresponding TEM images were also shown in Fig. 2B. Afterwards, GNPs-cDNA was prepared for amplification of telomerase activity assay, detailed preparation steps were shown in the supporting information. The rationale of this sensing system was verified in Fig. 2C. After the TS primer incubated with dNTPs and A549 cells/mL, GNPs-cDNA was injected, the Δ*F* reached to -100.9 Hz (curve a). As a control, when only dNTPs (curve b) or A549 cells (curve c) was added in the presence of TS primer, no obvious frequency shift was observed after the injection of GNPs-cDNA, implying the change of the Δ*F* for GNPs-cDNA was induced by the telomerase extension reaction product. Extended TS primer with repeating sequences of $(TTAGGG)_n$ could hybrid with GNPs-cDNA, resulting in a significant Δ*F*. Without GNPs-cDNA, no obvious Δ*F* was observed in the presence of TS primer, dNTPs and A549 cells (curve d), proving that the frequency shift of the solution was induced by the hybridization of extended TS primer and GNPs-cDNA. Therefore, these experiments verified the feasibility of the proposed sensor for evaluation of telomerase activity based on the signal amplification of GNPs-cDNA.

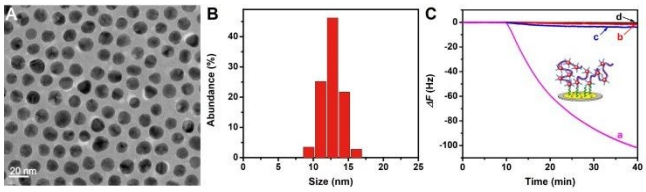

Fig. 2 (A) TEM image and (B) size distributions used GNPs. (C) Real-time frequency shifts of amplified QCM biosensor to control samples: (a) in the presence of dNTPs, target telomerase and GNPs-cDNA; (b) in the presence of dNTPs and GNPs-cDNA; (c) in the presence of target telomerase and GNPs-cDNA; (d) in the presence of dNTPs and target telomerase. 3000 A549 cells/mL was used.

Scanning electron microscopy (SEM) images were used to characterize the modification of QCM chip (Fig. 3). Fig. 3A showed the immobilized telomerase extension product on the QCM chip without GNPs-cDNA probes. Fig. 3B showed the chip surface modified with TS primer after the flush with GNPs-cDNA. Almost no GNPs were observed. Fig. 3C corresponded to the chip with telomerase extension product after the flush with GNPs-cDNA. A large number of GNPs were observed as the elongated TS primer would hybridize with GNPs-cDNA. This result also proved that GNPs-cDNA was indeed effective to increase the QCM sensitivity for telomerase detection. AFM imaging was used to characterize the hybridization of GNPs-cDNA on mica surface. Fig. 3D showed that the blank mica surface was smooth. While numerous "islands" were observed

on the mica surface when elongated TS primer was hybridized with GNPs-cDNA (Fig. 3E). The agreement of these data clearly indicated the specificity of the designed QCM method for telomerase detection.

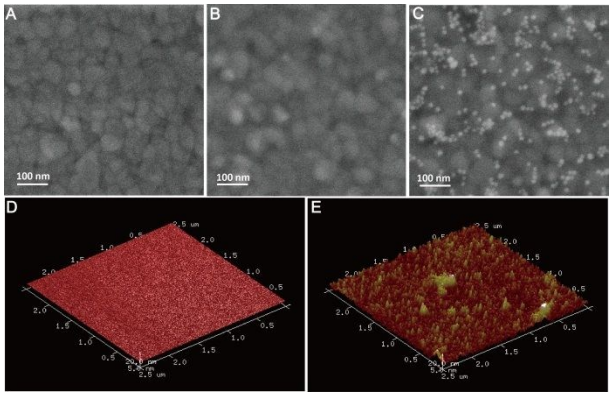

Fig. 3 SEM images of the chip surface of a QCM sensor. Chip surface of telomerisation product without GNPs-cDNA (A). Chip surface after GNPs-cDNA amplification in the absence (B) and presence of (C) telomerase reaction. AFM image of unmodified mica surface (D). The AFM image of mica surface after GNPs-cDNA amplification in the presence of telomerisation reaction (E).

Concentrations of TS primer and GNPs-cDNA were optimized. Fig. S1A and S1B showed that 40 nM TS primer and 20 nM GNPs-cDNA were optimal conditions. Under optimal conditions, various concentrations of A549 cells were added into the reaction system. As shown in Fig. 4A, when the concentration of A549 cells increased from 15 to 11000 cells/mL, the Δ*F* decreased obviously. The reason was that more telomerase produced more elongated TS primer in the presence of dNTPs, as a result, they hybridized with more GNPs-cDNA. In a word, the hybridization of telomerase extension product with GNPs-cDNA in the detection system was highly depended on the concentration of A549 cells. As shown in Fig. 4B, the frequency shift of GNPs-cDNA increased sharply at first and then levelled off. As shown in the inset plot, the Δ*F* shows a good linear fit with the concentration of A549 cells ranging from 100 to 7800 cells/mL. The linear equation was calibrated as Δ*F* = -29.86 - 0.024*C* (R^2=0.997), where *C* represented the concentration of A549 cells. A calculated detection limit was 37 A549 cells/mL. As shown in Table S2, the method is superior to the most of the methods previously reported, such as fluorescence,[8] electrochemical method,[22] UV-Vis,[31] and so on.

Fig. 4 (A) Real-time frequency shift of the amplified QCM biosensor for telomerase detection. From a to i: 0, 15, 100, 1500, 3000, 4500, 6000, 7800, 11000 A549 cells/mL. (B) Calibration curves of the frequency shift *vs* different concentration of A549 cells. Insets: Linear relationship between the Δ*F* and the concentration of A549 cells ranging from 100 to 7800 A549 cells/mL. Error bars show the standard deviation of three experiments.

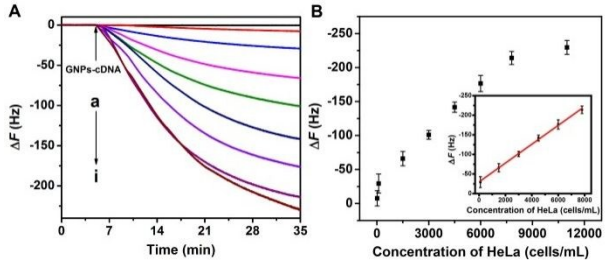

Contrast experiments were performed to test the practicality and selectivity of the present QCM sensor towards telomerase. As shown in Fig. S2, three kinds of cancer cell lines were used to detect telomerase activity extracted from other cancer cell lines. The frequency shift increased significantly for A549, HeLa, and MCF-7 cells but was negligible for heated A549 cells, indicating that the strategy could be used to detection of telomerase activity in all of these cell lines. Additionally, negligible Δ*F* was observed by replacing telomerase with L-Glutathione (GSH), poly(ADP-ribose) polymerase-1 (PARP-1) and horseradish peroxidase (HRP). This result indicated that the proposed QCM strategy exhibited good selectivity for telomerase detection due to the high specificity of the telomerase on TS primer extension reaction.

Inhibiting telomerase in tumors can result in telomere shortening to increase the efficacy of chemotherapy in cancer treatment.[32] In order to verify that the developed QCM method could be employed for the assessment and screening of telomerase inhibitors, BIBR1532 and curcumin were used as the model inhibitor. Results showed that the mass-dependent Δ*F* increased gradually with the increasing concentration of inhibitors and began to level off (Fig. S3). 3000 A549 cells/mL was used. This indicated that BIBR1532 and curcumin inhibited the telomerase activity efficiently. The obtained IC50 value of BIBR1532 and curcumin were 278 nM and 9.53 uM, respectively, which was in good agreement with previous studies.[33, 34] This result indicated that the proposed assay could be used to screen telomerase inhibitors. This is important for the new anti-cancer drug development. The inhibition efficiency (%) was calculated by the following formula:

$$\text{Inhibition (\%)} = \frac{\Delta F_2 - \Delta F_1}{\Delta F_2 - \Delta F_0} \times 100\%$$

Where ΔF_0 is the frequency change obtained from GNPs-cDNA without telomerase, ΔF_1 is the inhibited frequency change obtained from GNPs-cDNA with 3000 A549 cells/mL and inhibitors, and ΔF_2 is the frequency change obtained from GNPs-cDNA with 3000 A549 cells/mL.

Bladder cancers represent the most common urinary tract cancer worldwide.[35] Thus, accurate and efficient way for diagnosing bladder carcinoma is urgently needed.[36] To demonstrate the potential application of the present QCM strategy in clinic diagnosis, six human urine samples including 1 normal, 1 vesical calculus and 4 bladder cancer patients were pre-treated and detected. A threshold of 5 Hz, the mean value calculated from fifty blank samples x three times the standard deviation, was used for evaluation of bladder cancer. Detection results were shown in Table 1, the frequency shift in water, normal individual or vesical calculus patient were lower than the threshold value, while it is higher than 100 Hz for all the bladder cancer urine samples. The higher frequency shift

corresponds to the severity degree of bladder cancers patient. Thus, this sensitive, facile, reliable, and noninvasive QCM method for telomerase detection offers great potential for bladder cancer development evaluation.

Table 1 Comparison of the results by clinical diagnosis and the proposed method.

No.	Patient ID	Clinical outcome	-Δ*F*	Judgment
1	Water	-	1.1	Negative
2	Normal	Normal	1.4	Negative
3	1003295831	Vesical calculus	4.3	Negative
4	1007677148	Bladder cancer	100.6	Positive
5	1007922178	Bladder cancer	123	Positive
6	1007045669	Bladder cancer	128	Positive
7	1007924814	Bladder cancer	187	Positive
8	1008455348	Bladder cancer	180.7	Positive

In a summary, we designed a sensitive QCM method for detection of telomerase based on GNPs-cDNA signal amplification. Telomerase extends $(TTAGGG)_n$ using the 3' end as a primer and forms a single stranded G-rich strand which could hybridize with GNPs-cDNA. A linear range from 100 to 7800 A549 cells/mL has been achieved with a detection limit of 37 A549 cells/mL. This method is more sensitive or comparable to mostly previously reported methods. Additionally, it has been applied to evaluate telomerase inhibitor efficiency and evaluate bladder cancer development, obtaining satisfactory results. The proposed strategy opens up new opportunities for the study of telomerase detection with high sensitivity, which has good prospect to be used for clinical diagnosis and drug development.

We gratefully appreciate the support from National Natural Science Foundation of China (21775019, 21635004 and 81730087), Fundamental Research Funds for the Central Universities and A Project Funded by the Priority Academic Program Development of Jiangsu Higher Education Institutions (Grant Nos. 2242018K3DN04), The Open Project of The Key Laboratory of Modern Toxicology of Ministry of Education, Nanjing Medical University (NMUMT201804), Postgraduate Research & Practice Innovation Program of Jiangsu Province (KYCX18_0130).

Notes and references

1 E. Hiyama, J. W. Shay, K. Hiyama, L. Gollahon, M. A. Piatyszek, T. Kataoka, K. Kuroi, T. Yokoyama and A. F. Gazdar, *JNCI: J. Natl. Cancer I.*, 1996, **88**, 116-122.
2 G. Eom, H. Kim, A. Hwang, H.-Y. Son, Y. Choi, J. Moon, D. Kim, M. Lee, E.-K. Lim, J. Jeong, Y.-M. Huh, M.-K. Seo, T. Kang and B. Kim, *Adv. Funct. Mater.*, 2017, **27**, 1701832.
3 N. W. Kim, M. A. Piatyszek, K. R. Prowse, C. B. Harley, M. D. West, P. L. Ho, G. M. Coviello, W. E. Wright, S. L. Weinrich and J. W. Shay, *Science*, 1994, **266**, 2011.
4 C. Wang, H. Yang, S. Wu, Y. Liu, W. Wei, Y. Zhang, M. Wei and S. Liu, *TrAC, Trends Anal. Chem.*, 2018, **105**, 404-412.
5 H. Yang, A. Liu, M. Wei, Y. Liu, B. Lv, W. Wei, Y. Zhang and S. Liu, *Anal. Chem.*, 2017, **89**, 12094-12100.
6 D. Wang, R. Guo, Y. Wei, Y. Zhang, X. Zhao and Z. Xu, *Biosens. Bioelectron.*, 2018, **122**, 247-253.
7 J. Wang, L. Wu, J. Ren and X. Qu, Nanoscale, 2014, **6**, 1661-1666.
8 M. Zheng, R. Zhang, X. Tian, Z. Liu and Z. Zhang, *Chem. Commun.*, 2019, **55**, 2035-2038.
9 X. Xu, L. Wang, K. Li, Q. Huang and W. Jiang, *Anal. Chem.*, 2018, **90**, 3521-3530.
10 H. Yang, F. Fu, W. Li, W. Wei, Y. Zhang and S. Liu, Chemical Science, 2019, 10, 3706 – 3714.
11 Y. Zhuang, C. Shang, X. Lou and F. Xia, *Anal. Chem.*, 2017, **89**, 2073-2079.
12 Y. Zhuang, M. Zhang, B. Chen, R. Duan, X. Min, Z. Zhang, F. Zheng, H. Liang, Z. Zhao, X. Lou and F. Xia, *Anal. Chem.*, 2015, **87**, 9487-9493.
13 F. Meng, H. Chai, X. Ma, Y. Tang and P. Miao, *J. Mater. Chem. B*, 2019, **7**, 1926-1932.
14 F. Meng, Y. Xu, W. Dong, Y. Tang and P. Miao, *Mikrochimica acta*, 2018, **185**, 398.
15 F. Meng, X. Chen, W. Cheng, W. Hu, Y. Tang and P. Miao, *ChemElectroChem*, 2019, **6**, 2000-2003.
16 L. Wang, T. Meng, G. Yu, S. Wu, J. Sun, H. Jia, H. Wang, X. Yang and Y. Zhang, *Biosens. Bioelectron.*, 2019, **124-125**, 53-58.
17 Y. Liu, M. Wei, X. Liu, W. Wei, H. Zhao, Y. Zhang and S. Liu, *Chem. Commun.*, 2016, **52**, 1796-1799.
18 X. Liu, M. Wei, Y. Liu, B. Lv, W. Wei, Y. Zhang and S. Liu, *Anal. Chem.*, 2016, **88**, 8107-8114.
19 L. Xu, S. Zhao, W. Ma, X. Wu, S. Li, H. Kuang, L. Wang and C. Xu, *Adv. Funct. Mater.*, 2016, **26**, 1602-1608.
20 M. Sun, L. Xu, P. Fu, X. Wu, H. Kuang, L. Liu and C. Xu, *Adv. Funct. Mater.*, 2016, **26**, 7352-7358.
21 R. Freeman, E. Sharon, C. Teller , A. Henning , Y. Tzfati and I. Willner, ChemBioChem, 2010, **11**, 2362-2367.
22 P. Ling, J. Lei, L. Jia and H. Ju, *Chem. Commun.*, 2016, **52**, 1226-1229.
23 D. Wang, W. Tang, X. Wu, X. Wang, G. Chen, Q. Chen, N. Li and F. Liu, *Anal. Chem.*, 2012, **84**, 7008-7014.
24 J. Rickert, A. Brecht and W. Göpel, *Biosens. Bioelectron.*, 1997, **12**, 567-575.
25 S. H. Chen, Y. C. Chuang, Y. C. Lu, H. C. Lin, Y. L. Yang and C. S. Lin, *Nanotechnology*, 2009, **20**, 215501.
26 Z. M. Dong, X. Jin and G. C. Zhao, *Biosens. Bioelectron.*, 2018, 106, 111-116.
27 P. He, L. Liu, W. Qiao and S. Zhang, *Chem. Commun.*, 2014, **50**, 1481-1484.
28 Q. Chen, W. Tang, D. Wang, X. Wu, N. Li and F. Liu, *Biosens. Bioelectron.*, 2010, **26**, 575-579.
29 R. Z. Hao, H. B. Song, G. M. Zuo, R. F. Yang, H. P. Wei, D. B. Wang, Z. Q. Cui, Z. Zhang, Z. X. Cheng and X. E. Zhang, *Biosens. Bioelectron*, 2011, **26**, 3398-3404.
30 H. D. Hill and C. A. Mirkin, Nature protocols, 2006, 1, 324-336.
31 X. Xu, M. Wei, Y. Liu, X. Liu, W. Wei, Y. Zhang and S. Liu, *Biosens. Bioelectron.*, 2017, **87**, 600-606.
32 Y. Shi, L. Sun, G. Chen, D. Zheng, L. Li and W. Wei, *Targeted Oncology*, 2015, **10**, 565-573.
33 E. Pascolo, C. Wenz, J. Lingner, N. Hauel, H. Priepke, I. Kauffmann, P. Garin-Chesa, W. J. Rettig, K. Damm and A. Schnapp, *J. Bio. Chem.*, 2002, **277**, 15566-15572.
34 S. Chakraborty, U. Ghosh, N. P. Bhattacharyya, R. K. Bhattacharya and M. Roy, *Mutat. Res., Fundam. Mol. Mech. Mutagen.*, 2006, **596**, 81-90.
35 M. Burger, J. W. F. Catto, G. Dalbagni, H. B. Grossman, H. Herr, P. Karakiewicz, W. Kassouf, L. A. Kiemeney, C. La Vecchia, S. Shariat and Y. Lotan, *Euro. Urol.*, 2013, **63**, 234-241.
36 R. Liu, Z. Tian, J. Wang, Z. Zhang and Y. Xu, *Int. Urol. Nephrol.*, 2012, **44**, 1375-1382.

View Article Online
DOI: 10.1039/C9CC02610J

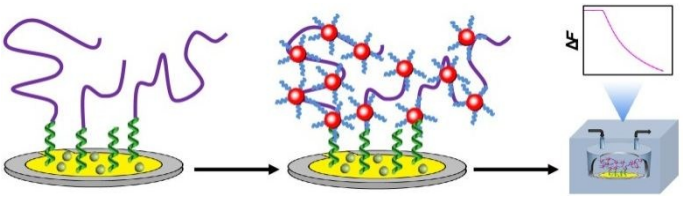

Mass-sensitive quartz crystal microbalance biosensor was constructed for telomerase sensing based on gold nanoparticles induced signal amplification